Numerical study of soliton scattering in inhomogeneous optical fibers

Yoji Kubota and Takashi Odagaki
Department of Physics, Kyushu University, Fukuoka 812-8581, Japan
(Received 21 August 2002; published 13 August 2003)

Using a variable-coefficient nonlinear Schrödinger equation, transmission profile of a single soliton in the optical fiber with an inhomogeneous region is studied numerically. It is found that the transmitted wave contains two solitons which form a bound state when the difference of the dispersion coefficient between the inhomogeneous and the homogeneous regions is large enough. When the amplitude of the transmitted wave is small, the transmitted wave is apt to contain a bound state soliton. With the increase of the length of the inhomogeneous region, a quantity E_3, which is the conserved quantity of the constant-coefficient nonlinear Schrödinger equation, for the transmitted wave converges to an asymptotic value with oscillation. It is found that the nonsoliton wave part of E_3 for the transmitted wave converges to an asymptotic value rapidly compared with other contributions to E_3. We find the condition for the parameters of the inhomogeneous region that a stable soliton can exist on the entire fiber.

DOI: 10.1103/PhysRevE.68.026603 PACS number(s): 42.81.Dp, 42.65.Tg, 05.45.Yv

I. INTRODUCTION

It is well known that optical fibers can support solitons on a balance of nonlinear effects and group velocity dispersion in anomalous dispersion regime. This fact was first predicted by Hasegawa and Tappert [1] and was demonstrated experimentally by Mollenauer *et al.* [2]. Since then, the soliton propagation in optical fibers has been widely studied from the interest of fundamental aspects and the potential for application to optical communication [3]. The propagation of solitons in optical fibers have been investigated theoretically using the nonlinear Schrödinger (NLS) equation.

In realistic optical fibers, characteristic parameters of the fiber are not constant but can depend on the location in the optical fiber. In other words, these parameters can have space-coordinate dependence. For example, the variations of the group velocity dispersion and the nonlinear coefficient are described by the variable-coefficient NLS (vNLS) equation. In these optical fibers, the incident soliton is modulated and is scattered by the inhomogeneity. Some properties of the vNLS equation have been studied [4–8]. When the coefficients of the vNLS equation satisfy a constraint, the equation possesses the Painlevé property [4,5], which relates to the integrability of the equation. Tian and Gao [6] found an auto-Bäcklund transformation and some special solutions to the vNLS equation, when its variable coefficients have a special relation. The modulational instability of the continuous wave in optical fibers was investigated and it was shown that the unstable spectral width is widened by random coefficient [7]. Grimshaw [8] used a multiple-scale method and constructed a soliton like solution for the vNLS equation varying slowly with the propagation.

In this paper, we consider the propagation of solitons in the optical fiber, where the group velocity dispersion has space-coordinate dependence. Considering a simple model, we investigate numerically the scattering of a single soliton due to an inhomogeneous region. This model will give some basic principles in the study of the soliton transmission, and the results of this model can be applied to more complicated situations. The main objective of this study is to investigate the behavior of transmitted waves, and it is found that the transmitted waves contain several solitons, some of which form a bound state. We clarify the condition for the transmitted waves to possess a bound state soliton. Note that Anderson *et al.* [9] studied soliton tunneling using a similar model to improve a single-soliton compression by a fiber, the dispersion of which changes stepwise.

The present paper is organized as follows. The model is introduced in Sec. II. In Sec. III, we explain the numerical method to calculate the parameters of solitons which emerge from the transmitted waves. In Sec. IV, numerical results are shown when a single soliton is injected into an inhomogeneous region of finite length. We investigate the dependence of the transmitted wave profile on the length of the inhomogeneous region and the intensity of nonuniformity. In Sec. V, we estimate the pulse shape of the transmitted waves for a very long inhomogeneous region by applying the results of Satsuma and Yajima [10] and compare this estimation with the results of the numerical calculation. Section VI is devoted to the discussion. Finally, in Sec. VII, we show that when the parameters of the optical fiber satisfy a certain condition, continuous waves do not emerge from the incident single soliton in the entire fiber, and the transmitted wave can propagate as a single soliton.

II. MODEL

We consider light pulses, which are linearly polarized, in an inhomogeneous optical fiber and study the evolution of its electric-field envelope A. The evolution of the envelope A is governed [3] by

$$i\frac{\partial A}{\partial z}+i\frac{1}{v_g}\frac{\partial A}{\partial t}-\frac{1}{2}\beta_2(z)\frac{\partial^2 A}{\partial t^2}+\gamma|A|^2A=0, \qquad (2.1)$$

where z is the distance of transmission along the fiber, t is the time, v_g is the group velocity of the light pulse, β_2 is the group velocity dispersion coefficient, and γ is the nonlinear coefficient which is inversely proportional to the effective core area. Coefficient β_2 is a real function of z. We restrict

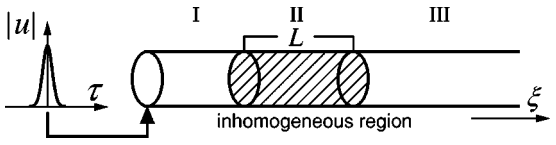

FIG. 1. The perspective of an incident soliton on the optical fiber with an inhomogeneous region (named region II), the length of which is L. Regions I and III are homogeneous regions.

ourselves to anomalous dispersion regime $\beta_2<0$, so that the optical fiber can support bright solitons.

We introduce dimensionless variables defined by

$$u=\sqrt{\frac{\gamma T_0^2}{|\tilde{\beta}_2|}}A,\quad \xi=\frac{|\tilde{\beta}_2|}{2T_0^2}z,\quad \tau=\frac{1}{T_0}(t-z/v_g), \tag{2.2}$$

where T_0 is the width of the incident pulse and $\tilde{\beta}_2$ is the group velocity dispersion coefficient of an ideal optical fiber which has no fluctuation. Here τ is the dimensionless delayed time. Under transformation (2.2), the equation of motion (2.1) is reduced to the vNLS equation

$$i\frac{\partial u}{\partial \xi}+a(\xi)\frac{\partial^2 u}{\partial \tau^2}+2|u|^2u=0, \tag{2.3}$$

where $a(\xi)=-\beta_2(z)/|\tilde{\beta}_2|$.

We consider optical fibers, a part of which has an elevated value of the group velocity dispersion β_2. We set

$$a(\xi)=\begin{cases}1 & \text{for } \xi\leqslant\xi_1 \text{ and } \xi_1+L\leqslant\xi\\ 1+\epsilon & \text{for } \xi_1<\xi<\xi_1+L,\end{cases} \tag{2.4}$$

where ϵ is interpreted as the intensity of nonuniformity, L is the dimensionless length of the inhomogeneous region scaled by $2T_0^2/|\tilde{\beta}_2|$. Since ξ_1 does not affect the results in our calculation, we set $\xi_1=1$ in the following calculation without loss of generality.

The NLS equation with a constant coefficient, $a(\xi)=1$ in Eq. (2.3), supports a single-soliton solution given by

$$u(\xi,\tau;\mu,\eta)=\eta\,\mathrm{sech}[\,\eta(\tau+\mu\xi)\,]\times\exp\left[-i\frac{\mu}{2}\tau-i\left(\frac{\mu^2}{4}-\eta^2\right)\xi\right], \tag{2.5}$$

where μ and η are arbitrary real parameters of the soliton and represent the velocity and the amplitude, respectively [11].

At the left end of the fiber $\xi=0$, we prepare a single soliton as the incident wave (Fig. 1). Without loss of generality we can set the parameters of the incident soliton, $\mu=0$ and $\eta=1$ (see Appendix A). We integrate numerically Eq. (2.3) over ξ using the second-order split-step Fourier method [3,12–14] imposing periodic boundary condition in τ. Since we prepare sufficiently large space of τ and finish the numerical calculation before waves reach the boundary in τ, the boundary condition does not affect the results. At $\xi=\xi_1$ and $\xi=\xi_1+L$, the conditions are imposed.

$$\lim_{\varepsilon\to+0}u(\xi_1+\varepsilon,\tau)=\lim_{\varepsilon\to+0}u(\xi_1-\varepsilon,\tau), \tag{2.6}$$

$$\lim_{\varepsilon\to+0}u(\xi_1+L+\varepsilon,\tau)=\lim_{\varepsilon\to+0}u(\xi_1+L-\varepsilon,\tau). \tag{2.7}$$

The NLS equation has an infinite set of constants of motion [11], among which the following three are well-known constants of motion:

$$E_1=\int|u|^2d\tau, \tag{2.8}$$

$$E_2=\int \mathrm{Im}\left[u\frac{\partial u^*}{\partial \tau}\right]d\tau, \tag{2.9}$$

$$E_3=\int\left(\left|\frac{\partial u}{\partial \tau}\right|^2-|u|^4\right)d\tau, \tag{2.10}$$

where the asterisk denotes complex conjugate. In the optical fiber under study, the constants of motion, E_1 and E_2, represent the energy and the mean frequency weighted by the intensity of optical pulses, respectively.

The quantities E_1 and E_2 are also conserved in the vNLS equation [8], and this can be proved by following the procedure of Pathria and Morris [15] for our model. Therefore, when discretization is used, the steps should be chosen so that E_1 and E_2 stay constant. These constants are determined by the incident wave and are given by $E_1=2$, $E_2=0$ in our paper.

On the other hand, E_3 is not conserved in the vNLS equation. Note that, in the conventional NLS equation where the time and the space coordinates are interchanged, E_3 is corresponds to the NLS Hamiltonian. We calculate this quantity E_3 for various parameters in later sections to quantify the effects of the inhomogeneity.

III. THE NUMBER OF SOLITONS

A. Inverse scattering method

Generally, a solution u to Eq. (2.3) consists of several solitons and dispersive wave continua. We denote the number of the solitons by N. Each soliton is characterized by two parameters μ_j and η_j $(j=1,\ldots,N)$. The solitons move with its characteristic velocity μ_j on the (τ,ξ) domain and the nonsoliton waves spread away as they propagate. Some solitons may have zero velocity, $\mu_j=0$, and we call these solitons ''stationary solitons.'' If some of the velocities μ_j [e.g., $j=1,\ldots,m(\leqslant N)$] are the same, these solitons can form a bound state, and it is called the m-bound soliton [11].

We use a method to calculate the parameters (μ_j,η_j) of the solitons which emerge from a wave u. According to the inverse scattering method [10,11,16], the NLS equation is associated to the eigenvalue equation

$$\hat{B}\Phi(\tau) \equiv \begin{pmatrix} i\frac{\partial}{\partial\tau} & u \\ -u^* & -i\frac{\partial}{\partial\tau} \end{pmatrix} \begin{pmatrix} \phi^{(1)}(\tau) \\ \phi^{(2)}(\tau) \end{pmatrix} = \zeta \begin{pmatrix} \phi^{(1)}(\tau) \\ \phi^{(2)}(\tau) \end{pmatrix}, \tag{3.1}$$

where u denotes a wave as a function of τ at an arbitrary ξ. It is known that the discrete eigenvalues ζ_j $(j=1,\ldots,N)$ with the positive imaginary part $[\mathrm{Im}(\zeta_j)>0]$ correspond to solitons and are related to the soliton parameters (μ_j,η_j) as

$$\zeta_j = \mu_j/4 + i\,\eta_j/2. \tag{3.2}$$

Since the eigenfunctions of the discrete eigenvalues are bounded, we impose the fixed boundary conditions on ϕ space to calculate the discrete eigenvalues in the following calculations.

B. Numerical method

In order to obtain eigenvalues of Eq. (3.1) numerically, we approximate the derivatives in Eq. (3.1) by the central difference [17]:

$$\begin{aligned} -b\,\phi^{(1)}_{n-1} + u_n\phi^{(2)}_n + b\,\phi^{(1)}_{n+1} &= \zeta\phi^{(1)}_n, \\ b\,\phi^{(2)}_{n-1} - u^*_n\phi^{(1)}_n - b\,\phi^{(2)}_{n+1} &= \zeta\phi^{(2)}_n, \end{aligned} \tag{3.3}$$

where $b=i/(2\Delta\tau)$. We define a matrix B by

$$\mathsf{B} = \begin{pmatrix} \ddots & \ddots & \ddots & & & 0 \\ 0 & 0 & u_{n-1} & b & & \\ b & u^*_{n-1} & 0 & 0 & -b & \\ & -b & 0 & 0 & u_n & b \\ & & b & u^*_n & 0 & 0 \\ 0 & & & \ddots & \ddots & \ddots \end{pmatrix}, \tag{3.4}$$

and denote its eigenvector and eigenvalue by $\Phi = (\ldots,\phi^{(1)}_{n-1},\phi^{(2)}_{n-1},\phi^{(1)}_n,\phi^{(2)}_n,\ldots)^T$ and ζ, respectively. Equation (3.1) is approximated by

$$\mathsf{B}\Phi = \zeta\Phi. \tag{3.5}$$

We note that it is shown below that there are fictitious discrete eigenvalues of the matrix B with positive imaginary part. It can be confirmed by substitution into Eq. (3.5) that the following vector

$$\Phi' = [\ldots,(-1)^n\phi^{(2)*}_n,(-1)^n\phi^{(1)*}_n,\ldots]^T$$

is also eigenvector of B for $-\zeta^*$. However, since the sequences $\{(-1)^n\phi^{(2)*}_n\}$ and $\{(-1)^n\phi^{(1)*}_n\}$ are not continuous as functions of n, this vector is not an approximant to the correct solution of Eq. (3.1). If the imaginary part of the eigenvalue ζ is positive, then the imaginary part of the eigenvalue $-\zeta^*$ is also positive, and there is fictitious eigenvalue $-\zeta^*$ with positive imaginary part.

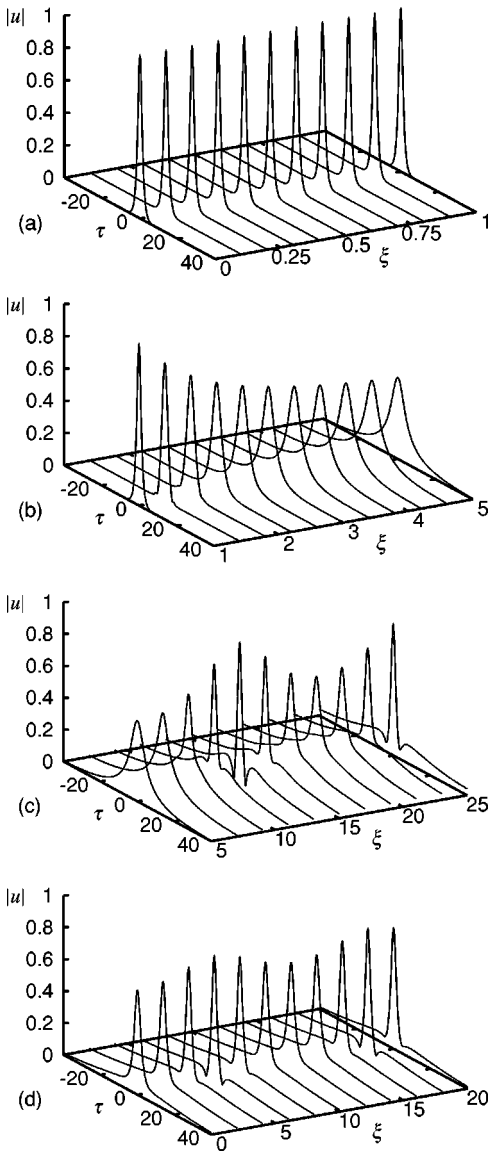

FIG. 2. The spatiotemporal evolution of waves $|u|$. τ is dimensionless delayed time and ξ is dimensionless distance of propagation. (a) The propagation of the wave in homogeneous region before the wave enters the inhomogeneous region, (b) in the inhomogeneous region, and (c) of the transmitted waves. (d) An exact 2-bound soliton of the NLS equation.

In Sec. IV, we calculate the eigenvalues of the matrix B numerically and ignore these fictitious solutions, so as to obtain the parameters (μ_j,η_j) of solitons.

IV. TRANSMITTED WAVES

A. Propagation through the inhomogeneous region

We integrated the vNLS equation, Eq. (2.3), over ξ numerically $L=4$ and $\epsilon=1$. We set $\Delta\tau\leqslant 0.1$ and the integration step $\Delta\xi\leqslant 0.001$ so that the conserved quantities E_1 and E_2 do not deviate from the values of the initial state. In Figs. 2(a–c), we show the amplitude of the wave $|u|$ as a function of τ and ξ, in three different regions of ξ.

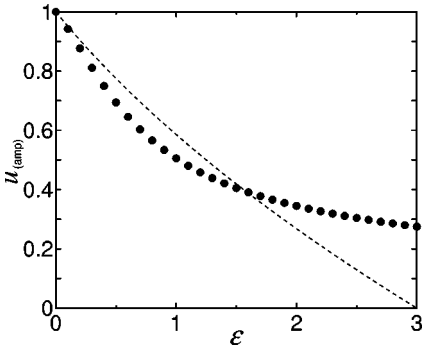

FIG. 3. The transmitted amplitude $u_{(amp)}$ (●) defined in Eq. (4.1) as a function of the intensity of nonuniformity ϵ. The dashed curve denotes the transmitted amplitude given by Eq. (5.6) when the inhomogeneous region is very long.

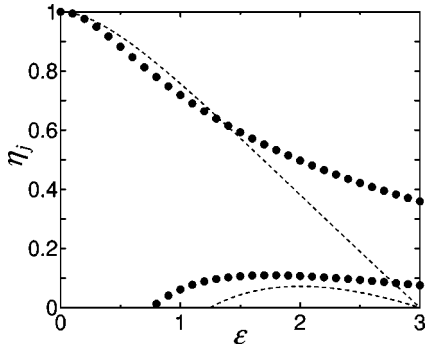

FIG. 4. The amplitude η_j (●) of the solitons for the transmitted waves are plotted as a function of the intensity of nonuniformity ϵ. The dashed curve denotes the soliton parameters given by Eqs. (5.8b) and (5.9b) when the inhomogeneous region is very long.

Figure 2(a) shows the propagation of the incident soliton in the homogeneous region (region I in Fig. 1) $\xi=[0,1]$. Since the incident soliton is the exact solution of Eq. (2.3) in region I, it propagates without decay.

In the inhomogeneous region (region II in Fig. 1), $\xi=[1,5]$, the wave propagates with its amplitude decreasing and its width widening [see Fig. 2(b)].

As can be seen from Fig. 2(c), the transmitted waves propagate with its shape varied in the homogeneous region III for $\xi>5$. We calculated the parameters (μ_j,η_j) of solitons for the transmitted waves numerically using the method described in Sec. III B. We found that the transmitted wave contains two solitons, the velocities of which are 0, and we conclude that these solitons form a stationary 2-bound soliton. The stationary 2-bound soliton with the same parameters are shown in Fig. 2(d) for comparison [18].

B. ϵ dependence

The properties of the transmitted waves were investigated for various intensities of nonuniformity ϵ keeping $L=4$ fixed.

The maximum amplitude of the transmitted waves which have just passed through the inhomogeneous region is defined by

$$u_{(\mathrm{amp})}=\max\{|u(\tau)|\}|_{\xi=\xi_1+L}. \tag{4.1}$$

We call this value ''transmitted amplitude'' and plot it as a function of ϵ in Fig. 3. It is seen from Fig. 3 that the transmitted amplitude decreases with the increase of ϵ.

The parameters (μ_j,η_j) of the solitons contained in the transmitted waves were calculated for various ϵ. We found that all the velocities μ_j of the solitons are 0. The amplitude η_j of transmitted solitons are shown in Fig. 4. It can be seen from Fig. 4 that when $\epsilon\gtrsim 0.8$, the transmitted waves contain a stationary 2-bound soliton.

Figure 5 shows the ϵ dependence of the quantity E_3 of the transmitted waves, which is conserved in a homogeneous region. E_3 increases with the increase of ϵ. We denote the soliton part of E_3 by $E_3^{(\mathrm{so})}$, which can be represented with the soliton parameters as

$$E_3^{(\mathrm{so})}=\sum_{j=1}^{N}\frac{1}{2}\eta_j\mu_j^2-\frac{2}{3}\eta_j^3. \tag{4.2}$$

Since the parameters (μ_j,η_j) of the solitons are constant in a homogeneous region, $E_3^{(\mathrm{so})}$ is constant in region III. We calculated $E_3^{(\mathrm{so})}$ for the transmitted waves using the parameters of the solitons shown in Fig. 4 and plot it in Fig. 5. The difference between E_3 and $E_3^{(\mathrm{so})}$ for large ϵ indicates that many nonsoliton waves emerge from the transmitted waves.

C. L dependence

We obtained the transmitted waves for various lengths L of the inhomogeneous region keeping the other parameter fixed at $\epsilon=1$.

The transmitted amplitude $u_{(\mathrm{amp})}$ is shown as a function of L in Fig. 6. When $L=0$, there is no inhomogeneous region, and the amplitude of the wave is the same as the one of the incident soliton. When $L\lesssim 2$, the transmitted amplitude $u_{(\mathrm{amp})}$ decreases rapidly with the increase of L. When $L\gtrsim 2$, the transmitted amplitude $u_{(\mathrm{amp})}$ oscillates around an asymptotic value and approaches it gradually with the increase of L.

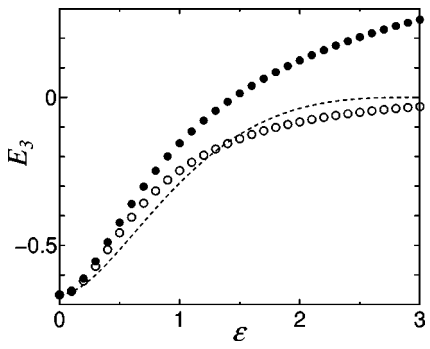

FIG. 5. The value E_3 (●) of the transmitted waves given by Eq. (2.10), and that value of the soliton part (○) of the transmitted waves are plotted against ϵ. The dashed curve denotes the soliton part of E_3 of the transmitted waves estimated in Sec. V for the long inhomogeneous region.

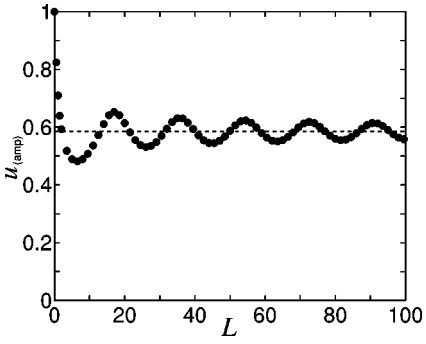

FIG. 6. The transmitted amplitude $u_{(\mathrm{amp})}$ (●) defined in Eq. (4.1) as a function of the length L of the inhomogeneous region. The dashed line denotes the transmitted amplitude given by Eq. (5.6) when the inhomogeneous region is very long.

The parameters (μ_j, η_j) of the transmitted solitons were calculated for various L. We plot those parameters (μ_j, η_j) in Figs. 7(a) and 7(b). It can be seen from these figures that there are four different cases of L. The transmitted waves contain the following.

(1) A stationary single soliton, $\mu_j = 0$.

(2) A stationary 2-bound soliton, $\mu_j = 0$.

(3) A stationary single soliton and two solitons whose velocities μ_j are not 0. These nonzero velocity solitons move away from the origin of τ axis and do not form a bound state soliton. We call these nonzero velocity solitons ''scattered solitons.''

(4) A stationary 2-bound soliton and two scattered solitons.

It can be seen from Fig. 7(b) that when $L \lesssim 3.0$, a stationary single soliton emerges from the transmitted waves [case (1)]. Case (2) occurs when $3.5 \lesssim L \lesssim 14$, and case (4) occurs at $L \sim 15$. When $16.0 \lesssim L \lesssim 24.0$, case (3) takes place, and cases (2), (4), and (3) take place in a sequential order with

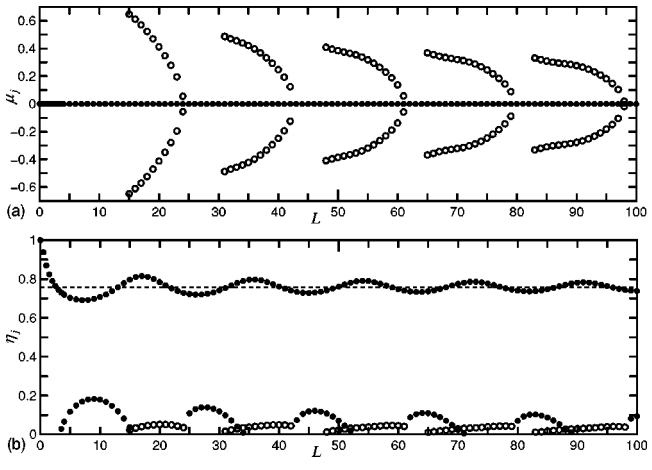

FIG. 7. The parameters (μ_j, η_j) of the transmitted solitons are plotted for various lengths L of the inhomogeneous region. (a) The velocity μ_j of each soliton. The solid circle (●) corresponds to $\mu_j = 0$ and the open circle (○) corresponds to $\mu_j \neq 0$. (b) The amplitude η_j of each soliton, the velocity μ_j of which is 0 (●) and is not 0 (○). The dashed line denotes the soliton parameters given by Eq. (5.8b) when the inhomogeneous region is very long.

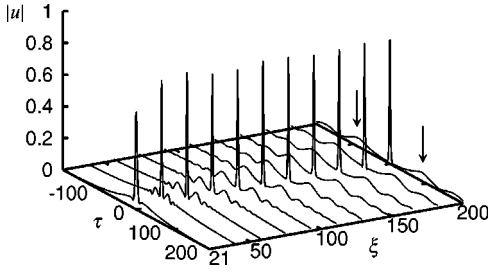

FIG. 8. The spatiotemporal evolution of the transmitted waves $|u|$. τ is dimensionless delayed time and ξ is the dimensionless distance of propagation. The length of the inhomogeneous region and the intensity of nonuniformity are $L = 20$ and $\epsilon = 1.0$, respectively. Small solitons are indicated by arrows.

the increase of L. It can also be seen from Fig. 7(b) that the amplitude η_j of the scattered solitons are small compared with that of the stationary solitons.

For example, for $\epsilon = 1$ and $L = 20$, the transmitted wave contains three solitons, each parameters of which are $(\mu_j, \eta_j) = (0.0, 0.7814)$ and $(\pm 0.4136, 0.0490)$, as is shown in Figs. 7(a) and 7(b). Since each soliton velocity μ_j is different, there is no bound state soliton [case (3)]. The transmitted waves $|u|$ are shown as a function of τ and ξ in Fig. 8. At $\xi = 21$, i.e., the boundary between regions II and III, the wave consists of a large peak pulse and broad tails. As the wave propagates, a set of small pulses emerge around the large pulse symmetrically [indicated by arrows in Fig. 8] and move away in the opposite direction. We verified that these small pulses are the scattered solitons by calculating the velocities of these small pulses on the (τ, ξ) domain.

The quantity E_3 can be represented as the sum of two contributions [19]:

$$E_3 = E_3^{(\mathrm{so})} + E_3^{(\mathrm{ns})}, \tag{4.3}$$

where $E_3^{(\mathrm{ns})}$ is the nonsoliton wave part of E_3. In a homogeneous region, since E_3 and $E_3^{(\mathrm{so})}$ are constants, this quantities $E_3^{(\mathrm{ns})}$ is also constant. These quantity E_3, $E_3^{(\mathrm{so})}$, and $E_3^{(\mathrm{ns})}$ of the transmitted waves for various L are shown in Fig. 9. The

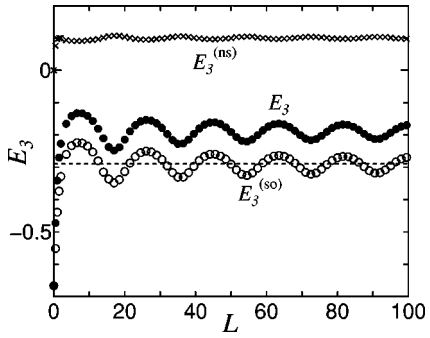

FIG. 9. The value E_3 (●) of the transmitted waves given by Eq. (2.10), the value of the soliton part $E_3^{(\mathrm{so})}$ (○) of the transmitted waves, and the value of the nonsoliton wave part $E_3^{(\mathrm{ns})}$ (×) of the transmitted waves are plotted against L. The dashed line denotes the soliton part of E_3 for the transmitted waves estimated in Sec. V for the long inhomogeneous region.

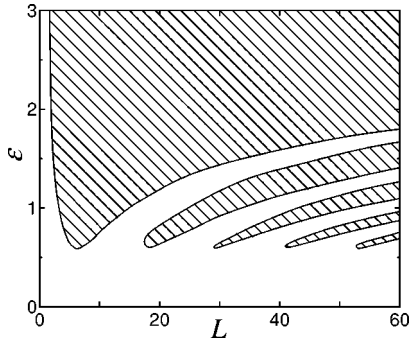

FIG. 10. Shaded areas denote the parameters L and ϵ for the cases where the 2-bound soliton emerge from the transmitted waves. Here L denotes the length of the inhomogeneous region and ϵ denotes the intensity of nonuniformity. These results are obtained by using the method described in Appendix B.

behavior of E_3 is similar to that of $E_3^{(\mathrm{so})}$, but E_3 approaches a different value. $E_3^{(\mathrm{ns})}$ approaches an asymptotic value rapidly and oscillates with smaller amplitude than that of E_3 and $E_3^{(\mathrm{so})}$. It would be possible to measure the inhomogeneity of optical fibers by this quantity $E_3^{(\mathrm{ns})}$.

D. 2-bound soliton

We identified the region in (τ,ξ) domain where a 2-bound soliton emerges, which is shown in Fig. 10. Here, for shortening the computational time, we use the method described in Appendix B to calculate the parameters of the transmitted solitons. As can be seen from this figure, a 2-bound soliton emerges from the transmitted waves only when $\epsilon \gtrsim 0.6$ and L is an appropriate length. It can be seen from Fig. 10 that for $\epsilon \lesssim 1.0$, the allowed region shrinks gradually with the increase of L.

V. ANALYSIS FOR LONG INHOMOGENEOUS REGION

A. Asymptotic behavior

We treat an asymptotic case where the length L of the inhomogeneous region (region II) is very long, $L \gg 1$, and estimate the profile of transmitted waves by using the analytical results of Satsuma and Yajima [10]. In Ref. [10], it is shown by the inverse scattering method that when a wave is represented as $Q\,\mathrm{sech}\,T$ on the NLS equation, the parameters (μ_j,η_j) of solitons contained in the wave $Q\,\mathrm{sech}\,T$ can be calculated exactly, and the nonsoliton part of the wave asymptotically decays as $\xi^{-1/2}$.

We consider the propagation of the solitons by dividing it into the three regions.

(1) The wave at the end of region I is given by

$$u = \mathrm{sech}\,\tau \exp(i\xi_1). \tag{5.1}$$

Since the phase factor of Eq. (5.1) can be absorbed into the eigenfunction in Eq. (3.1), the phase factor of Eq. (5.1) can be ignored [20], and for the same reason we ignore a phase factor in u hereafter.

(2) In region II, the following transformation of variables:

$$U = \frac{1}{C}u, \quad Z = C^2(\xi - \xi_1), \quad T = \tau, \tag{5.2}$$

reduces the vNLS equation and Eq. (5.1) to

$$i\frac{\partial U}{\partial Z} + \frac{\partial^2 U}{\partial T^2} + 2|U|^2 U = 0, \tag{5.3}$$

$$U = \frac{1}{C}\,\mathrm{sech}\,T \quad \text{at} \quad Z = 0, \tag{5.4}$$

where C is the constant given by $C = \sqrt{1+\varepsilon}$.

We apply the results in Ref. [10] to our model system. When $-5/9 \leqslant \epsilon < 3$, a single soliton emerges in region II. The nonsoliton waves disappear when $Z \gg 1$. On the assumption that region II is sufficiently long, $L \gg 1$, the nonsoliton waves can be ignored, and there is only the single soliton at the end of region II, where $Z(=C^2L) \gg 1$. The single soliton at the end of region II is represented as

$$u = (2-\sqrt{1+\epsilon})\,\mathrm{sech}\left[\left(2\sqrt{\frac{1}{1+\epsilon}} - 1\right)\tau\right]. \tag{5.5}$$

The transmitted amplitude $u_{(\mathrm{amp})}$ for very long region II is given by

$$u_{(\mathrm{amp})}^{(L\gg 1)} = 2 - \sqrt{1+\epsilon}. \tag{5.6}$$

(3) The NLS equation is invariant under the transformation of variables:

$$U' = \frac{1}{C'}u, \quad Z' = C'^2\xi, \quad T' = C'\tau, \tag{5.7}$$

where C' is an arbitrary constant. Here, we set $C' = (2/\sqrt{1+\epsilon}) - 1$, and the wave which enters region III is reduced to $U' = \sqrt{1+\epsilon}\,\mathrm{sech}\,T'$.

We use the results in Ref. [10] again, then the parameters of the transmitted soliton for $-5/9 \leqslant \epsilon \leqslant 5/4$ are given by

$$\mu_1 = 0, \tag{5.8a}$$

$$\eta_1 = C'(2\sqrt{1+\epsilon} - 1), \tag{5.8b}$$

and when $5/4 < \epsilon < 3$, a 2-bound soliton emerges in region III, the parameters of which are given by Eqs. (5.8), and

$$\mu_2 = 0, \tag{5.9a}$$

$$\eta_2 = C'(2\sqrt{1+\epsilon} - 3). \tag{5.9b}$$

Note that Eq. (5.8b) is consistent with the relation derived in Ref. [9].

These quantities estimated for $L \gg 1$ are compared with the numerical results obtained in Sec. IV below.

B. Comparison with the numerical results

1. ϵ dependence

In Fig. 3, we compare the transmitted amplitude $u_{(\mathrm{amp})}^{(L\gg 1)}$ for very long region II, i.e., $L\gg 1$, with the transmitted amplitude $u_{(\mathrm{amp})}$ of the numerical results for $L=4$. It can be seen from this figure that $u_{(\mathrm{amp})}$ and $u_{(\mathrm{amp})}^{(L\gg 1)}$ are similar when $\epsilon\ll 1$, and show significant difference when ϵ is large.

The parameters (μ_j, η_j) of the transmitted solitons for $L\gg 1$ are shown in Fig. 4. In this case, the 2-bound soliton emerges for $\epsilon > 5/4$. It should be noticed that this critical value of ϵ is different from the one obtained in the numerical calculation in Sec. IV B, due to difference of the length L of region II. This difference of the critical value of ϵ will be discussed in Sec. VI B.

2. L dependence

The transmitted amplitude $u_{(\mathrm{amp})}^{(L\gg 1)}$ for $L\gg 1$ is compared with the numerical results $u_{(\mathrm{amp})}$ for $\epsilon=1$ in Fig. 6. It is shown in this figure that the transmitted amplitude $u_{(\mathrm{amp})}$ oscillates around the asymptotic value $u_{(\mathrm{amp})}^{(L\gg 1)}$ and approaches it with L.

It is shown in Sec. V A that when $L\gg 1$ and $\epsilon=1$, the transmitted soliton is a stationary single soliton, and we show the amplitude η_1 of its soliton in Fig. 7(b). It can, however, be seen from the numerical results in this figure that a stationary 2-bound soliton emerges in region III for some limited values of L. Figure 7(b) shows that with increase in L, the larger amplitude η_j of the soliton gradually approaches the asymptotic value with oscillation, and the smaller amplitude η_j of the soliton emerges and disappears repeatedly and gradually decay with a much slower rate.

The asymptotic value of $E_3^{(\mathrm{so})}$ estimated for $L\gg 1$ is obtained by using Eqs. (5.8) and (4.2), and is shown in Fig. 9. It can be seen from this figure that $E_3^{(\mathrm{so})}$ decays to the asymptotic value with oscillation.

VI. DISCUSSION

A. Development into the asymptotic soliton

When ϵ is small, $|\epsilon|\ll 1$, the evolution of the wave in the inhomogeneous region (region II) has been investigated by the dispersive perturbation [21] and the variational technique [22]. Here, we consider how the incident wave develops into the single soliton in region II intuitively.

The amplitude of the wave at an appropriate point ξ_2 in region II is given by $u_{(\mathrm{amp})}$ for shorter region II, where $L=\xi_2-\xi_1$, and the dependence of $u_{(\mathrm{amp})}$ on L are shown in Fig. 6. In region II, the amplitude of the wave oscillates around the asymptotic value $u_{(\mathrm{amp})}^{(L\gg 1)}$ and approaches it as the wave propagates.

Roughly speaking, these phenomena are interpreted as follows: In region I, the incident soliton propagates without decay, and this fact indicates that contributions of the derivative term and the nonlinear term in the vNLS equation [Eq. (2.3)] to the incident soliton are balanced. When the wave enters region II, the derivative term and the nonlinear term in the vNLS equation are off balanced, and the wave is in a nonstationary state since the coefficient $a(\xi)$ in the vNLS equation is larger in region II than the one in region I. The wave evolves into the soliton asymptotically, and this phenomenon can be considered as the wave converging to a stationary state. Therefore, the values of the derivative term and the nonlinear term in the vNLS equation vary as the wave propagates so as to be balanced. Since the wave must satisfy the conservation law [Eq. (2.8)], the amplitude of the wave decreases so that the wave becomes wider and smoother [see Fig. 2(b)]. However, the amplitude of the wave overdamps beyond the asymptotic amplitude since the effect of the nonlinear term is strengthened by the existence of the nonsoliton wave, and then the wave approaches the asymptotic form again. The amplitude of the wave behaves like a damped oscillator with the distance of the propagation in region II.

B. 2-bound soliton

In Secs. IV and V, we have seen that a 2-bound soliton emerges from the transmitted waves for some limited values of the fiber parameters. It can be assumed from those results that a 2-bound soliton is contained in a wave when the wave has entered a region where $a(\xi)$ is smaller than the one of the preceding region. Here, we consider the condition for the emergence of a 2-bound soliton from a wave and ensure the above assumption.

We consider two successive regions. In a region A, $a(\xi)=a_1$, and in a region B, $a(\xi)=a_2(\neq a_1)$, where a_1 and a_2 are arbitrary positive constants. We assume that region A is long enough so that a wave u develops into a stationary soliton near the end of region A. It can be calculated by using Eq. (2.5) and Eqs. (5.2) where we set $C=\sqrt{a_1}$ that the single soliton at the end of region A can be represented by

$$u=\sqrt{a_1}\,\eta\,\mathrm{sech}(\eta\tau), \tag{6.1}$$

where η is an appropriate positive constant. Since the injected wave in region B is of hyperbolic secant shape, it is well known [3] that the number of the solitons (N) can be obtained by

$$N^2=\gamma|A|^2T_0^2/|\beta_2|. \tag{6.2}$$

In this case, the number of the solitons is given by $N=\sqrt{a_1/a_2}$ [cf. Eqs. (2.1) and (2.2)]. We conclude that when region A is sufficiently long, the number of the solitons in region B is determined by the ratio of value $a(\xi)$ in each region and a bound state soliton emerges in region B when a_2 is sufficiently smaller than a_1.

It is shown in Sec. V A that the estimation for a very long inhomogeneous region indicates that a 2-bound soliton emerges from the transmitted waves for $\epsilon > 5/4$. It should be noticed that for finite length L, a 2-bound soliton can emerge even when $\epsilon \leqslant 5/4$ and the critical value also depends on L (see Fig. 10). It can be seen from Figs. 6 and 7(b) that a 2-bound soliton emerges from the transmitted waves when $u_{(\mathrm{amp})}$ is small.

These facts are interpreted as follows. We consider two fibers (named fiber F_I and fiber F_{II}) under consideration

with different lengths of the inhomogeneous region, L_1 and $L_2(>L_1)$, but with the same value ϵ of the inhomogeneity. We denote the wave at the right edge of the inhomogeneous region by $f_1(\tau)$ and $f_2(\tau)$, respectively, and the ratio of the amplitude of $f_1(\tau)$ and $f_2(\tau)$ by $R=\max[f_2(\tau)]/\max[f_1(\tau)]$. We assume $R<1$ (or $R>1$). We note that the wave $f_1(\tau)$ is given by the wave at $\xi=\xi_1+L_1$ in the inhomogeneous region of fiber F_{II}. When a wave propagates in the inhomogeneous region of fiber F_{II}, the wave is varied gradually with the distance of the transmission, ξ. We now assume that $f_2(\tau)$ is given by the same function as $f_1(\tau)$ with an appropriate scaling of the amplitude and the width. Since the wave must satisfy the conservation law [Eq. (2.8)], the wave $f_2(\tau)$ can be represented as

$$f_2(\tau)=Rf_1(R^2\tau). \tag{6.3}$$

It has been explained in Sec. III A that the number of the solitons contained in the wave $f_2(\tau)$ is calculated by substituting Eq. (6.3) into u in Eq. (3.1). It can be shown from Eq. (3.1) and Eqs. (5.7) with $C'=R^2$ that the number of solitons contained in $f_2(\tau)$ is the same one which are calculated for $u=(1/R)f_1(\tau)$. We conclude that when the transmitted amplitude of the wave $f_2(\tau)$ is R times smaller (or larger) than the one of the wave $f_1(\tau)$, the height of the potential u in Eq. (3.1) is effectively $1/R$ times higher (or lower) than that of $f_1(\tau)$. The transmitted wave with the smaller amplitude might have a bound state soliton.

VII. EXACTLY SOLVABLE CASE

We set the parameter for the intensity of nonuniformity,

$$\epsilon=-\left(1-\frac{1}{n^2}\right), \tag{7.1}$$

where n is a positive integer, so that Eq. (5.4) is reduced to $U=n\,\mathrm{sech}\,T$. In this case, no nonsoliton waves emerge in the inhomogeneous region, and the incident wave propagates as an exact soliton in the inhomogeneous region [10]. When n is larger than 1, the wave is the exact n-bound soliton and its envelope pulsates periodically with the frequency $\pi/[4(1+\epsilon)]$ along with the propagation [20]. Since the incident soliton revives its shape periodically, the transmitted wave is the same as the incident one when the length of the inhomogeneous region is

$$L=\frac{\pi}{4(1+\epsilon)}m, \tag{7.2}$$

where m is a positive integer, and it propagates as an exact single soliton in the homogeneous region III.

Thus, the incident soliton propagates as exact solitons in the entire fiber by setting the fiber parameters as Eqs. (7.1) and (7.2).

VIII. SUMMARY AND CONCLUSION

We have investigated numerically the propagation of solitons in the optical fiber with an inhomogeneous region. We summarize the profile of the transmitted waves as follows: It is found that when ϵ is small, the profile of the transmitted wave is well approximated by the asymptotic form in the limit of long region. With the increase of ϵ, the property of the transmitted waves deviates from the one of the incident soliton. For large ϵ, the transmitted waves contain a 2-bound soliton.

We have obtained the nonsoliton wave contribution $E_3^{(\mathrm{ns})}$ to the quantity E_3. We have found that $E_3^{(\mathrm{ns})}$ approaches an asymptotic value rapidly with the increase of L, and it would be possible to measure the inhomogeneity of optical fibers by this quantity $E_3^{(\mathrm{ns})}$.

The small solitons with nonzero velocity (scattered solitons) emerge from the transmitted waves for some limited values of the fiber parameters. It may be necessary to consider the emergence of those scattered solitons in some applications of the soliton.

It is shown by the asymptotic estimation for $L\gg 1$ that the 2-bound soliton emerges from the transmitted waves when $\epsilon>5/4$. It is interesting to note that for some limited values of finite lengths of inhomogeneous regions, a 2-bound soliton emerges even for $\epsilon\leqslant 5/4$. This fact indicates that we can generate a 2-bound soliton by controlling the length of the inhomogeneous region for smaller ϵ.

We have considered the condition for generating a 2-bound soliton when a wave has passed through a boundary of two successive regions. When the first region is sufficiently long, the number of the solitons in the second region is determined by the ratio of the coefficients $a(\xi)$ of the vNLS equation in both regions. When the first region is not long enough for the wave to converge to the asymptotic form, the wave at the end of the first region depends on both the intensity of $a(\xi)$ and the length of the first region. We have concluded that the wave contains many solitons in subsequent region when the amplitude of the wave is small at the end of the first region.

ACKNOWLEDGMENTS

This work was supported by the JSPS and in part by a Grant-in-Aid for Scientific Research from the Ministry of Education, Culture, Sports, Science, and Technology.

APPENDIX A: RENORMALIZATION OF THE INCIDENT SOLITON PARAMETERS

In this appendix we explain the reason that the parameters of the incident soliton can be set as $\mu=0$ and $\eta=1$, without loss of generality. When the parameters of the incident soliton are set as $\mu=\mu_0$ and $\eta=\eta_0$, where μ_0 and η_0 are arbitrary constants, we use the following transformation of variables:

$$u'=\frac{1}{\eta_0}u\exp\left[i\frac{\mu_0}{2}\tau+i\frac{\mu_0^2}{4}\int_0^{\xi}a(\xi'')d\xi''\right], \tag{A1a}$$

$$\tau'=\eta_0\tau+\mu_0\eta_0\int_0^{\xi}a(\xi'')d\xi'', \tag{A1b}$$

$$\xi' = \eta_0^2 \xi. \tag{A1c}$$

Then, the incident soliton is reduced to the soliton with parameters $\mu = 0$ and $\eta = 1$.

However, the transformation of variables changes the scale of the length, and then length L of the inhomogeneous region is varied. This variation of L can be absorbed in the L dependence of the transmission profile.

Therefore, assuming that the parameters (μ, η) of the incident soliton are chosen arbitrary constants, these cases can be reduced to the case where the incident soliton parameters are $\mu = 0$ and $\eta = 1$.

APPENDIX B: AN ALTERNATE METHOD FOR NUMERICAL CALCULATION

We introduce an alternate method to calculate numerically the discrete eigenvalues of the matrix B defined in Eq. (3.4), which coincide with the parameters of solitons (see in Sec. III). We can calculate only the parameters of stationary solitons (velocity μ_j is 0) by this method; however, we can get results fast with less memory compared with calculating the eigenvalues of B directly.

In general, the secular equation

$$\det(\mathsf{B} - \lambda \mathsf{E}) = 0 \tag{B1}$$

is accurate if λ is an eigenvalue of the matrix B, where E denotes an unit matrix. In our model system, when we calculate the parameters of the stationary soliton, we search for the eigenvalues of B only in $[0,i]$ on the imaginary axis by the following three reasons.

(1) Since the eigenvalues which correspond to solitons have positive imaginary parts, we search for eigenvalues only in the upper half plane $\mathrm{Im}(\lambda) > 0$.

(2) The energy [Eq. (2.8)] can be rewritten as

$$E_1 = \sum_{j=1}^{N} 2\eta_j + E_1^{(\mathrm{ns})}, \tag{B2}$$

where $E_1^{(\mathrm{ns})}$ is the energy of nonsoliton waves [11,20]. The energy is a positive constant $E_1 = 2$ [see Sec. II] throughout the calculation. The amplitude η_j of solitons is positive. It can be seen from Eq. (2.8) that $E_1^{(\mathrm{ns})}$ is non-negative. Therefore, each term in Eq. (B2) is non-negative; and it is found that the amplitude η_j of solitons, which is derived from the incident soliton, is less than or equal to 1. Since the amplitude η_j of the soliton is the imaginary part of the discrete eigenvalue [see Eq. (3.2)], we search for the discrete eigenvalues in $\mathrm{Im}(\lambda) \leqslant 1$.

(3) The velocity of stationary soliton is $\mu_j = 0$, and the velocity μ_j of the soliton is the real part of eigenvalue [see Eq. (3.2)]. We search eigenvalues only in the imaginary axis on the complex λ plane.

Therefore, we can concentrate in $\det(\mathsf{B} - \lambda \mathsf{E})$ changing λ in $[0,i]$ on the imaginary axis to calculate the parameters of the stationary solitons.

[1] A. Hasegawa and F.D. Tappert, Appl. Phys. Lett. **23**, 142 (1973).
[2] L.F. Mollenauer, R.H. Stolen, and J.P. Gordon, Phys. Rev. Lett. **45**, 1095 (1980).
[3] G.P. Agrawal, *Nonlinear Fiber Optics*, 2nd ed. (Academic Press, New York, 1995).
[4] N. Joshi, Phys. Lett. A **125**, 456 (1987).
[5] P.A. Clarkson, Proc. R. Soc. Edinburgh, Sect. A: Math. **109**, 109 (1988).
[6] Y.-T. Gao and B. Tian, Comput. Math. Appl. **40**, 1107 (2000); B. Tian and Y.-T. Gao, *ibid.* **31**, 115 (1996).
[7] J. Garnier and F.K. Abdullaev, Physica D **145**, 65 (2000).
[8] R. Grimshaw, Proc. R. Soc. London, Ser. A **368**, 377 (1979).
[9] D. Anderson, M. Lisak, B. Malomed, and M. Quiroga-Teixeiro, J. Opt. Soc. Am. B **11**, 2380 (1994).
[10] J. Satsuma and N. Yajima, Suppl. Prog. Theor. Phys. **55**, 284 (1974).
[11] V.E. Zakharov and A.B. Shabat, Zh. Eksp. Teor. Fiz. **61**, 118 (1971) [Sov. Phys. JETP **34**, 62 (1972)].
[12] J.A.C. Weideman and B.M. Herbst, SIAM (Soc. Ind. Appl. Math.) J. Numer. Anal. **23**, 485 (1986).
[13] T.R. Taha and M.J. Ablowitz, J. Comput. Phys. **55**, 203 (1984).
[14] A.D. Bandrauk and H. Shen, J. Phys. A **27**, 7147 (1994).
[15] D. Pathria and J.L. Morris, Phys. Scr. **39**, 673 (1989).
[16] Y.-C. Ma and M.J. Ablowitz, Stud. Appl. Math. **65**, 113 (1981).
[17] C.F. Gerald and P.O. Wheatley, *Applied Numerical Analysis*, 3rd ed. (Addison-Wesley, Reading, MA, 1984), Chap. 6.
[18] H.A. Haus and M.N. Islam, IEEE J. Quantum Electron. **QE-21**, 1172 (1985).
[19] Y.S. Kivshar and B.A. Malomed, Rev. Mod. Phys. **61**, 763 (1989)
[20] Y. Kodama and A. Hasegawa, Int. J. Quantum Chem. **QE-23**, 510 (1987).
[21] M.W. Chbat *et al.*, J. Opt. Soc. Am. B **10**, 1386 (1993).
[22] W.L. Kath and N.F. Smyth, Phys. Rev. E **51**, 1484 (1995).